

## Orbital Ordering and Jahn-Teller Distortion in Perovskite Ruthenate SrRuO<sub>3</sub>

Horng-Tay Jeng,<sup>1,2</sup> Shi-Hsin Lin,<sup>2</sup> and Chen-Shiung Hsue<sup>2</sup>

<sup>1</sup>Institute of Physics, Academia Sinica, Taipei 11529, Taiwan

<sup>2</sup>Department of Physics, National Tsing Hua University, Hsinchu 300, Taiwan

(Received 7 October 2004; published 8 August 2006; publisher error corrected 8 August 2006)

Local density approximation plus on-site Coulomb interaction  $U$  band structure calculations reveal that SrRuO<sub>3</sub> exhibits a half-metallic ground state with an integer spin moment of  $2.0\mu_B/\text{SrRuO}_3$ . An associated tilting  $4dt_{2g}$  orbital ordering on a Ru sublattice is observed under the on-site Coulomb interaction  $U$  in the presence of lattice distortion. This finding unravels the on-site Coulomb correlation as the driving force of the  $4d$  orbital ordering and Jahn-Teller distortion as well as of the half-metallic ground state.

DOI: 10.1103/PhysRevLett.97.067002

PACS numbers: 74.70.Pq, 71.20.-b

Orbital, charge, spin, and lattice degrees of freedom play important roles in the electronic, magnetic, and transport properties of transition-metal oxides. It was proposed half a century ago that orbital ordering (OO) is closely related to magnetic and crystallographic lattices in perovskite manganites such as La<sub>1-x</sub>Ca<sub>x</sub>MnO<sub>3</sub> in the low temperature insulating charge ordered phase [1]. In recent years, the phenomenon of charge ordering has been observed in perovskite [2] and magnetite [3]. Direct observation of OO in La<sub>0.5</sub>Sr<sub>1.5</sub>MnO<sub>3</sub> using soft x-ray diffraction measurements [4] has also been reported. The OO states are usually found in  $3de_g$  manganite systems where the cooperative Jahn-Teller (JT) distortions are significant due to the strong hybridization between the  $e_g$  and O2p electrons [5]. Evidence for  $t_{2g}$  OO with higher degeneracy and relatively weaker JT distortions is also found in localized  $3d$  systems such as titanates [6], vanadates [7], and magnetite [8], whereas  $4dt_{2g}$  OO state is also proposed for relatively itinerant layered ruthenate Ca<sub>2</sub>RuO<sub>4</sub> [9,10].

Ruthenium-based oxides have attracted increasing attention in recent years because of the interesting electronic and magnetic properties and the newly discovered unconventional superconductivity in layered ruthenate Sr<sub>2</sub>RuO<sub>4</sub> [11]. Substitution of Ca<sup>2+</sup> for Sr<sup>2+</sup> ions in Sr<sub>2</sub>RuO<sub>4</sub> leads to an antiferromagnetic Mott insulator [12]. The nearly cubic perovskite SrRuO<sub>3</sub> is the only known ferromagnetic ( $T_c \approx 160$  K) metal among the  $4d$  transition-metal oxides, whereas the metallic and magnetic properties are significantly suppressed in CaRuO<sub>3</sub> [13]. It is usually believed that  $4d$  electrons are relatively itinerant so that electron correlation in Ru-based oxides is less important than that in  $3d$  oxides [14–16]. Nevertheless, measurements on specific heat [14], optical properties [17], infrared and optical reflectivity [18], thermal, magnetic, and transport properties [19], and photoemission and x-ray absorption spectroscopy [20–24] of SrRuO<sub>3</sub> all indicate that the electron correlation effects in Ru4d orbitals is important and should be taken into consideration.

SrRuO<sub>3</sub> crystallizes in an orthorhombic perovskite structure with 4 f.u. per cell [25]. As shown in Fig. 1, the

lattice distortion involves JT distortions in the crystal  $ab$  plane as well as rotation and zigzag tilting of RuO<sub>6</sub> octahedra along the  $c$  axis. In the ionic model, the four  $4d$  electrons of the Ru<sup>4+</sup> ion occupy the  $t_{2g}$  triplet and leave the higher  $e_g$  doublet empty under the octahedral crystal field. In accordance with Hund's rule, Ru<sup>4+</sup> is in the high spin state with the spin alignment of ( $t_{2g}^3 \uparrow, t_{2g}^1 \downarrow$ ), giving rise to a moment of  $2\mu_B/\text{f.u.}$  and a half-metallic ground state with the majority spin insulating and minority spin conducting. In contrast, calculations using local density approximation (LDA) give a metallic ground state with a relatively small spin moment ranging from 0.9 to  $1.6\mu_B/\text{Ru}$  [14,15,26]. On the other hand, the wide range of the measured saturation magnetization from 0.8 to  $1.6\mu_B/\text{Ru}$  [27–29] is attributed to the high magnetocrystalline anisotropy and the difficulty in obtaining saturation in SrRuO<sub>3</sub> [29]. A saturation magnetization of  $2\mu_B$  could be obtained by extrapolating to the high field limit [29].

In this work, we present electronic structure calculations within the framework of LDA with generalized gradient

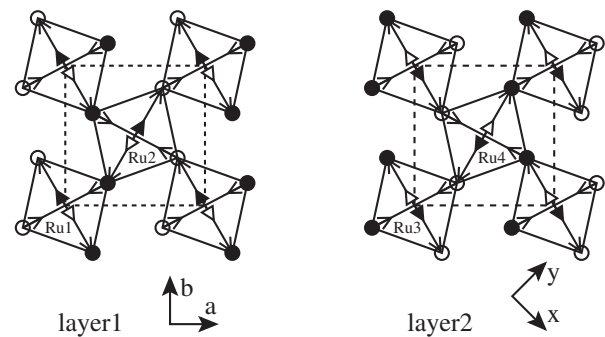


FIG. 1. Lattice structure and JT distortions of SrRuO<sub>3</sub>. Solid and open circles denote planar O in the unit cell (dashed line) with, respectively, upward and downward displacements (along the  $c$  axis). Solid and open triangles are, respectively, the apex O above and below the Ru ions. The arrows indicate the direction of planar distortions with respect to the RuO<sub>apex</sub> bond length. The deformation is exaggerated by 3 times.  $abc$  and  $xyz$  are, respectively, the crystal and local coordinates.

correction (GGA) plus on-site Coulomb interaction  $U$  (LDA +  $U$ ) [30] using the refined orthorhombic crystal structure [25]. We find not only a half-metallic ground state in consistence with the ionic model, but also an associated tilting  $4dt_{2g}$  OO on the Ru sublattice closely related to the JT distortions. To our knowledge, there is no experimental observation on the OO of SrRuO<sub>3</sub>. The calculations were performed on 100  $k$  points over the irreducible Brillouin zone with a cutoff energy of 400 eV for plane waves using the full-potential projected augmented wave method [31] as implemented in the VASP package [32]. Coulomb energy  $U = 3.5$  eV and exchange parameter  $J = 0.6$  eV [33] were used for Ru ions to explore the correlation effects in  $4d$  electrons.

Figures 2(a) and 2(b) show the density of states (DOS) of SrRuO<sub>3</sub> from GGA and LDA +  $U$ , respectively. Similar to previous LDA results [14,15], GGA gives a metallic ground state with the spin-up  $Ru t_{2g}$  band  $\sim 0.5$  eV below and the spin-down  $Ru t_{2g}$  band  $\sim 0.3$  eV above the Fermi level [Fig. 2(a)]. Photoemission and x-ray absorption spectroscopy observed a lower occupied  $Ru t_{2g}$  band  $\sim 1.1$  eV below and a higher unoccupied  $Ru t_{2g}$  band  $\sim 0.5$  eV above the Fermi level [20], indicating electron correlation effects. Taking into account the on-site  $U$ , the spin-up  $t_{2g}$  orbital is relatively localized with a suppressed bandwidth and a lower band energy, whereas the spin-down  $t_{2g}$  band is pushed upwards slightly [Fig. 2(b)]. The LDA +  $U$   $t_{2g} \uparrow$  band at  $\sim 1.1$  eV below and  $t_{2g} \downarrow$  band at  $\sim 0.7$  eV above the Fermi level are in better agreement with the observed band energies [20]. Moreover, the spin-up  $t_{2g}$  band is hence fully occupied and the Fermi level lies in the enhanced energy gap, giving rise to a half-metallic ground state in consistence with the valence configuration ( $t_{2g}^3 \uparrow, t_{2g}^1 \downarrow$ ) of Ru from ionic model. This is to be compared with the high spin polarization of 50%–60% observed through point-contact Andreev reflection experiments [34–36], which is much larger than 26% from GGA [Fig. 2(a)] and 9%–20% from LDA [14,15].

A total moment of  $1.90\mu_B/\text{f.u.}$  is given from GGA with only  $1.11\mu_B$  (58%) located within the nonoverlapping Ru

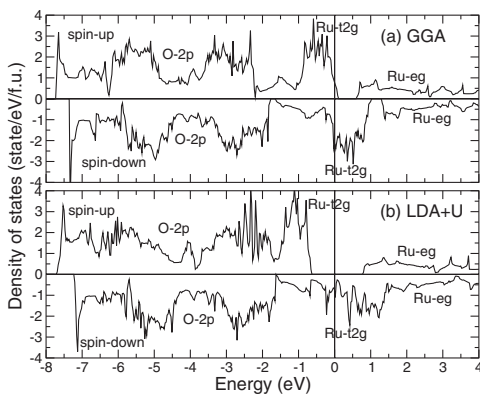


FIG. 2. DOS of SrRuO<sub>3</sub> from (a) GGA and (b) LDA +  $U$ . The Fermi level is at the zero energy.

atomic sphere of radius 1.0 Å. Similar partitions of spin moment at the Ru site (64%–67%) [14–16] have also been found using LDA. An integer moment of  $2.0\mu_B/\text{f.u.}$  for the half-metallic ground state is given from LDA +  $U$  with  $1.20\mu_B$  (60%) at the Ru site. The obtained moment of Ru is consistent with the measured saturation magnetization ranging from 0.8 to  $1.6\mu_B/\text{Ru}$  [27–29], while the total moment of SrRuO<sub>3</sub> from LDA +  $U$  agrees with that given from ionic model and with the saturation moment extrapolated to the high field limit [29]. Because of the significant  $p$ - $d$  hybridization between the relatively extended Ru $4d$  and O $2p$  orbitals, there exists a nontrivial moment of  $0.15\mu_B$  at the O site from both GGA and LDA +  $U$ . In all cases investigated, neither charge nor spin ordering is found in SrRuO<sub>3</sub> (the charge and spin separations being less than  $0.03e$  and  $0.03\mu_B$ , respectively).

To identify the OO state in SrRuO<sub>3</sub>, we present in Fig. 3 the DOS projected onto the five  $4d$  orbitals of the four Ru ions in the local coordinates ( $xyz$ ) with the  $z$  axis directed to the crystal  $c$  axis and the  $x$  and  $y$  axes pointing to the crystal  $[1\bar{1}0]$  and  $[110]$  directions, respectively (Fig. 1). In the minority spin channel (Fig. 3), all the Ru ions exhibit  $t_{2g}$  bands right below the Fermi level down to  $\sim -1.6$  eV with reduced DOS at the Fermi level. The four Ru ions can be divided into two groups according to the orbital characters of the partially occupied spin-down  $t_{2g}$  bands. These bands of Ru1 and Ru3 [Figs. 3(a) and 3(c)] are of predominate  $d_{xz}$  and  $d_{xy}$  characters, whereas those of Ru2 and Ru4 [Figs. 3(b) and 3(d)] are of mainly  $d_{yz}$  and  $d_{xy}$  features. Within the Ru atomic spheres of radii 1.0 Å, the integrated charges of these  $t_{2g}$  bands are  $0.73e$  with 58% of  $d_{xz}$  in the former and  $0.75e$  with 59% of  $d_{yz}$  in the latter. These results indicate the formation of a spin-down  $4dt_{2g}$  OO state in the Ru sublattice that each Ru has approximately one spin-down electron occupying a mixed  $t_{2g}$  orbital. This mixed orbital is a combination of two of the  $t_{2g}$  orbitals with the third  $t_{2g}$  orbital empty. Such an OO state results from the fluctuations of occupancies among the threefold  $t_{2g}$  orbitals provided in LDA +  $U$  and is

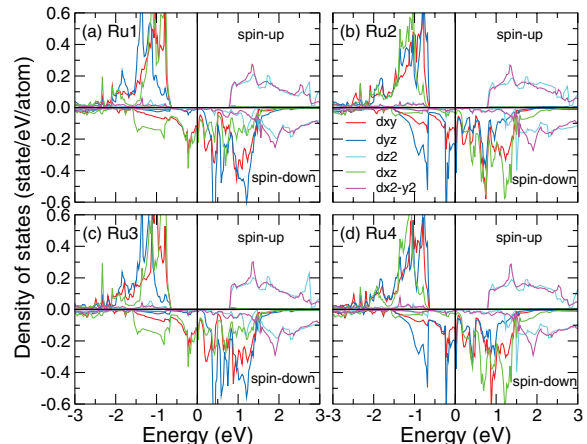


FIG. 3 (color). DOS of Ru in SrRuO<sub>3</sub> from LDA +  $U$ .

closely related to the cooperative JT distortions as discussed below.

Figure 4 illustrates the isosurface of charge density ( $0.15e/\text{\AA}^3$ ) corresponding to the spin-down  $t_{2g}$  bands below the Fermi level ( $-1.6-0.0$  eV) [Fig. 2(b)]. The OO pattern is clearly seen that there exists a canted crosslike charge density distribution on each  $\text{Ru}^{4+}$  with the distribution on Ru1 and Ru3 belonging to one group, while with that on Ru2 and Ru4 belonging to another. Combined with the zigzag tilting of the  $\text{RuO}_6$  octahedra along the  $c$  axis, the charge distributions on Ru1 and Ru3 arrange in zigzag “ribbons” running parallel to the  $c$  axis, whereas the zigzag ribbons on the Ru2-Ru4 sublattice differ from the former by a  $90^\circ$  rotation about the  $c$  axis. Taking Ru1, for example, the JT distortions with shortened Ru1-O bond lengths ( $1.94$  \AA) along the  $y$  axis and elongated bond lengths ( $2.04$  \AA) along the  $x$  axis (Fig. 1) split the threefold  $t_{2g}$  orbitals into the lower  $d_{xz}$  and higher  $d_{yz}$  and  $d_{xy}$  orbitals. The tilting of  $\text{RuO}_6$  octahedron (Fig. 1) includes two kinds of displacements in different directions: the apex O ions deform along the  $x$  axis (Ru-O<sub>apex</sub> bond lengths =  $1.98$  \AA), whereas two of the coplanar O move upwards and two move downwards along the  $c$  axis. Such distortions would lower the Coulomb repulsion between the O ions and the observed inclined  $\text{Ru}d_{xz}$  electron cloud, which is a combination of  $d_{xz}$  and  $d_{xy}$  orbitals as demonstrated in Fig. 4. In return, the inclined  $d_{xz}$  orbital with the four lobes pointing towards the intermediate directions in between each three of the neighboring O anions would further stabilize the lattice distortion. The LDA +  $U$  calculations show that the total energy of  $\text{SrRuO}_3$  in the distorted orthorhombic OO state is  $0.20$  eV/f.u. lower than that in the ideal cubic structure without OO.

Recent x-ray absorption spectroscopy measurement on the orbital population of a Ru ion in  $\text{Ca}_2\text{RuO}_4$  reveals approximate 0.5 and 1.5 holes in the  $d_{xy}$  and  $d_{yz/zx}$  orbitals,

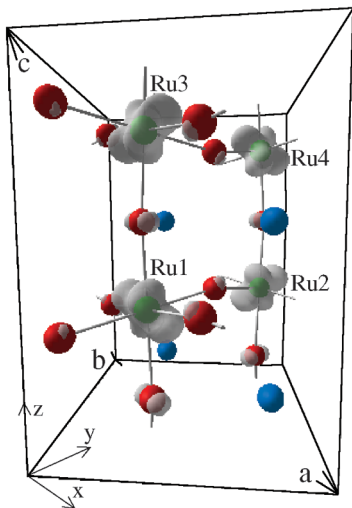


FIG. 4 (color). OO of  $\text{SrRuO}_3$ . Blue, green, and red balls are, respectively, Sr, Ru, and O ions. The origin has been shifted to  $(-1/3, -1/3, -1/3)$ .

respectively [37]. Calculations using the LDA +  $U$  method [10] and the Hubbard model [9] obtained, respectively, a tetragonal  $d_{xy}$  OO and a complicate OO pattern with a doubled unit cell for the ground state of  $\text{Ca}_2\text{RuO}_4$ . Interestingly, the population of the canted OO found for  $\text{SrRuO}_3$ , in which about half of  $d_{xy}$  and half of  $d_{xz}$  (or  $d_{yz}$ ) orbitals are occupied, agrees with the hole population observed in  $\text{Ca}_2\text{RuO}_4$  [37]. Similar measurement would clarify the OO of  $\text{SrRuO}_3$ .

Another significant issue is whether the spin-orbit (SO) interaction would destroy the observed OO in  $\text{SrRuO}_3$ . Without SO coupling, the octahedral crystal field makes the cubic harmonics a nature basis set and gives rise to the lower  $t_{2g}$  and higher  $e_g$  bands. A distorted octahedral crystal field hence provides a possibility for OO as discussed previously. Nonetheless, the SO interaction, which couples the spin to the angular momentum of the charge distribution and hence the crystal structure, prefers the spherical harmonic basis set. As a result, the competitive SO coupling tends to mix the cubic harmonic basis and could ruin the observed OO. By including the SO interaction self-consistently in the LDA +  $U$  calculations, we found that in spite of the relatively strong SO coupling in  $4d$  orbitals, the site and orbital decomposed DOS (Fig. 3) and the OO pattern (Fig. 4) remain more or less the same due to the extended  $\text{Ru}4d$  orbitals and the strong octahedral crystal field. The obtained total energy is  $0.13$  eV/ $\text{SrRuO}_3$  lower with a quenched orbital magnetic moment of  $0.03\mu_B/\text{Ru}$ . A similar trend has also been found in  $\text{Ca}_2\text{RuO}_4$  [38] that even with the SO coupling, the crystal field on Ru ions is strong enough to quench the orbital moment and to stabilize the OO.

Importantly, the formation of the  $\text{Ru}4d$  OO state occurs only when the on-site Coulomb interaction  $U$  and structural distortion are taken into account simultaneously. Calculations in the absence of either on-site  $U$  or lattice distortion give rise to a normal ground state with the spin-down electron distributed evenly onto the three  $t_{2g}$  orbitals. Calculations with on-site  $U$  taken as a parameter varying from  $1.0$  to  $5.5$  eV reveal that the OO is established with  $U \geq 2.5$  eV, and a larger  $U$  gives rise to a cleaner OO. The half-metallic band structures exist with  $U \geq 1.5$  eV, while a higher  $U$  tends to further suppress the DOS at the Fermi level in the minority spin. An energy gap of  $0.1$  eV in the minority spin is opened with  $U = 5.0$  eV, which would make  $\text{SrRuO}_3$  a Mott-Hubbard insulator. On the other hand, lattice relaxation under  $U = 3.5$  eV further stabilizes the orbital ordered half-metallic ground state by  $0.24$  eV/f.u. with suppressed lattice distortions ( $\Delta\text{RuO} = 1\%-1.5\%$ ) similar to the measured one ( $\Delta\text{RuO} = 2\%-3\%$ ) [25]. Thus, the obtained orbital ordered half-metallic ground state is robust upon varying  $U$ , lattice relaxation, and even upon including the SO interaction in the calculations.

To understand surface effects on the OO of  $\text{SrRuO}_3$ , we performed LDA +  $U$  slab calculations under lattice relaxation. For the  $\text{SrO}$ -terminated case, the electronic structures

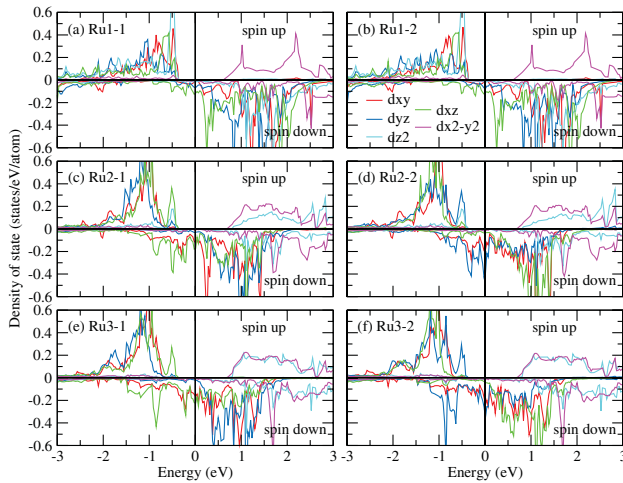


FIG. 5 (color). LDA +  $U$  DOS of Ru in relaxed SrRuO<sub>3</sub> surface layers. Ru1, Ru2, and Ru3 indicate the first (surface), second, and third RuO<sub>2</sub> layer, respectively. Two Ru ions in each layer are depicted in the left and right panels.

are similar to those of the bulk calculations (not shown here). This is presumably due to the fully ionic characters of Sr<sup>2+</sup> and O<sup>2-</sup>, and therefore the relatively stable close shell states. In contrast, in the RuO<sub>2</sub>-terminated case, there exist significant deviations in DOS of the surface layer as shown in Fig. 5. Associated with the outwards displacement (0.18 Å) of the surface layer, one of the unoccupied spin-up  $e_g$  bands is energetically lowered from  $\sim 1.5$  to  $\sim -0.5$  eV [Figs. 5(a) and 5(b)]. This nontrivial band shift is due to the octahedral symmetry breaking at the surface Ru, in which the spin-up  $d_{z^2}$  band energy is lowered in the absence of one of the apex O and the enhancement of the other Ru-O<sub>apex</sub> bond length. Combined with the bulk  $t_{2g}$  band at  $\sim -1.1$  eV, such an extra occupied band at  $\sim -0.5$  eV provides an explanation on the newly observed double-peak feature at  $\sim -1.1$  and  $\sim -0.4$  eV [23,24,39]. Furthermore, because of the enhanced Coulomb repulsion from the occupied spin-up  $d_{z^2}$  electron, the spin-down  $t_{2g}$  bands are noticeably raised over the Fermi level so that the ionicity of Ru remains about the same. This surface-induced electron redistribution also leads to the enhanced magnetic moment of  $2.24\mu_B$  per surface Ru, which is much larger than  $1.20\mu_B/\text{Ru}$  in the bulk calculation. We note that despite the drastic orbital rearrangement at the surface Ru, the OO presented above for the bulk state remains more or less the same in the inner layers [Figs. 3 and 5(c)–5(f)].

In summary, we have investigated the electronic structures of SrRuO<sub>3</sub> in the distorted orthorhombic structure using LDA +  $U$ . The obtained band energies agree well with those from photoemission and x-ray absorption spectroscopy. We also found that the spin-down electrons of Ru form a  $4dt_{2g}$  OO state by occupying, respectively, the canted  $d_{xz}$  and  $d_{yz}$  orbitals of Ru1-Ru3 and Ru2-Ru4 sublattices. Our finding unravels the nature of the OO,

the close connection to the JT distortions, and the importance of the on-site correlation  $U$  in the relatively extended Ru4d orbitals.

We thank H. C. Ku and B. N. Lin for valuable discussions. This work was supported by the National Science Council of Taiwan.

- [1] J. B. Goodenough, Phys. Rev. **100**, 564 (1955).
- [2] J. Q. Li *et al.*, Phys. Rev. Lett. **79**, 297 (1997).
- [3] J. P. Wright, J. P. Attfield, and P. G. Radaelli, Phys. Rev. Lett. **87**, 266401 (2001).
- [4] S. B. Wilkins *et al.*, Phys. Rev. Lett. **91**, 167205 (2003).
- [5] Y. Tokura and N. Nagaosa, Science **288**, 462 (2000).
- [6] J. Hemberger *et al.*, Phys. Rev. Lett. **91**, 066403 (2003).
- [7] G. R. Blake *et al.*, Phys. Rev. Lett. **87**, 245501 (2001).
- [8] H. T. Jeng, G. Y. Guo, and D. J. Huang, Phys. Rev. Lett. **93**, 156403 (2004).
- [9] T. Hotta and E. Dagotto, Phys. Rev. Lett. **88**, 017201 (2002).
- [10] J. H. Jung *et al.*, Phys. Rev. Lett. **91**, 056403 (2003).
- [11] Y. Maeno *et al.*, Nature (London) **372**, 532 (1994).
- [12] C. S. Alexander *et al.*, Phys. Rev. B **60**, R8422 (1999).
- [13] M. Shepard *et al.*, J. Appl. Phys. **81**, 4978 (1997).
- [14] P. B. Allen *et al.*, Phys. Rev. B **53**, 4393 (1996).
- [15] D. J. Singh, J. Appl. Phys. **79**, 4818 (1996).
- [16] I. I. Mazin and D. J. Singh, Phys. Rev. B **56**, 2556 (1997).
- [17] J. S. Ahn *et al.*, Phys. Rev. Lett. **82**, 5321 (1999).
- [18] P. Kostic *et al.*, Phys. Rev. Lett. **81**, 2498 (1998).
- [19] G. Cao *et al.*, Phys. Rev. B **56**, 321 (1997).
- [20] K. Fujioka *et al.*, Phys. Rev. B **56**, 6380 (1997).
- [21] J. Okamoto *et al.*, Phys. Rev. B **60**, 2281 (1999).
- [22] J. Park *et al.*, Phys. Rev. B **69**, 085108 (2004).
- [23] J. Kim, J. Chung, and S.-J. Oh, Phys. Rev. B **71**, 121406(R) (2005).
- [24] M. Takizawa *et al.*, Phys. Rev. B **72**, 060404(R) (2005).
- [25] M. Shikano *et al.*, Solid State Commun. **90**, 115 (1994).
- [26] P. Ravindran *et al.*, Solid State Commun. **124**, 293 (2002).
- [27] A. Callaghan, C. W. Moeller, and R. Ward, Inorg. Chem. **5**, 1572 (1966).
- [28] J. M. Longo, P. M. Raccach, and J. B. Goodenough, J. Appl. Phys. **39**, 1327 (1968).
- [29] A. Kanbayasi, J. Phys. Soc. Jpn. **41**, 1876 (1976); **44**, 89 (1978); **44**, 108 (1978).
- [30] A. I. Liechtenstein, V. I. Anisimov, and J. Zaanen, Phys. Rev. B **52**, R5467 (1995).
- [31] G. Kresse and D. Joubert, Phys. Rev. B **59**, 1758 (1999).
- [32] G. Kresse and J. Furthmüller, Phys. Rev. B **54**, 11169 (1996).
- [33] I. V. Solovyev, P. H. Dederichs, and V. I. Anisimov, Phys. Rev. B **50**, 16861 (1994).
- [34] P. Raychaudhuri *et al.*, Phys. Rev. B **67**, 020411 (2003).
- [35] B. Nadgorny *et al.*, Appl. Phys. Lett. **82**, 427 (2003).
- [36] J. Sanders *et al.*, J. Appl. Phys. **97**, 10C912 (2005).
- [37] T. Mizokawa *et al.*, Phys. Rev. Lett. **87**, 077202 (2001).
- [38] Z. Fang, N. Nagaosa, and K. Terakura, Phys. Rev. B **69**, 045116 (2004).
- [39] LDA gives no  $t_{2g}$  band lower than  $-0.5$  eV in slab calculations, and therefore is not able to reproduce the experimentally observed double-peak feature.